

Generic Contrast Agents

Our portfolio is growing to serve you better. Now you have a *choice*.



[VIEW CATALOG](#)

AJNR

This information is current as of May 24, 2025.

Correlations of Hippocampal Atrophy and Focal Low-Frequency Magnetic Activity in Alzheimer Disease: Volumetric MR Imaging-Magnetoencephalographic Study

Alberto Fernández, Juan Arrazola, Fernando Maestú, Carlos Amo, Pedro Gil-Gregorio, Christian Wienbruch and Tomás Ortiz

AJNR Am J Neuroradiol 2003, 24 (3) 481-487

<http://www.ajnr.org/content/24/3/481>

Correlations of Hippocampal Atrophy and Focal Low-Frequency Magnetic Activity in Alzheimer Disease: Volumetric MR Imaging–Magnetoencephalographic Study

Alberto Fernández, Juan Arrazola, Fernando Maestú, Carlos Amo, Pedro Gil-Gregorio, Christian Wienbruch, and Tomás Ortiz

BACKGROUND AND PURPOSE: Patients with Alzheimer disease (AD) have more low-frequency activity on conventional EEG and increased focal magnetoencephalographic (MEG) dipole density (DD) in delta and theta bands. This activity concurs with atrophy and reduced metabolic and perfusion rates, particularly in temporoparietal structures. The relationship between functional and structural measures and their conjoined capability to improve the diagnosis of AD were assessed in this study.

METHODS: Whole-head MEG recordings were obtained in 15 patients in whom the diagnosis of AD had been made and in 16 healthy control subjects during a resting condition. MR imaging volumetric data were also obtained; these included global cerebral, temporal lobe, and hippocampal volumes.

RESULTS: DD in the delta and theta bands was enhanced in the AD group compared with the healthy control subjects. Slow-wave activity differed significantly between the groups in the temporoparietal regions of both hemispheres. Left hippocampal volume was correlated with left temporal and parietal delta DD and left temporal theta DD. A combination of left hippocampal volume and left temporal theta DD enabled correct classification in 87.1% of the patients with AD or control subjects.

CONCLUSION: Results support the predominant role of temporoparietal hypofunction as defined by DD and hippocampal structural deficits shown on MR images in patients with AD. A multidisciplinary perspective of different techniques may improve our understanding of the disease and our diagnostic abilities.

Alzheimer disease (AD) is a complex neurodegenerative disorder that should be investigated from a multidisciplinary perspective. Nevertheless, the most common research procedures rely on the capability of a single technique to distinguish between patients with AD and age-matched healthy control subjects. Several studies demonstrate how functional-metabolic measures (ie, positron emission tomography

[PET] or single photon emission tomography [SPECT]) reveal a stable portrait of AD; this includes a prominent pattern of temporoparietal (association cortex) and, eventually, hippocampal hypometabolism-hypoperfusion (1–7). For instance, the sensitivity of SPECT in distinguishing patients with AD reportedly ranges from 43% to 100% (5, 8). This broad range depends on the diagnostic criteria and the severity of the disease, with more severe disease being identified more easily.

Similar findings appear in EEG recordings. Here, an increase of slow activity, usually focused in the temporoparietal regions (9, 10), together with decreased activity in the alpha band, are considered the prototypical characteristics of AD (11). Jonkman (12) performed an exhaustive review of the accuracy of EEG in distinguishing patients with AD from control subjects from 16 reports published between 1983 and 1995 and found that the rate of correct identification ranges from 54% to 100%, with a median of 81%.

Received August 6, 2002; accepted after revision September 27.

From the Center for Magnetoencephalography Dr Pérez Modrego, Universidad Complutense de Madrid (A.F., F.M., C.A., T.O.) and the Departments of Neuroradiology (J.A.) and Geriatrics (P.G.-G.), Hospital Universitario San Carlos, Madrid, Spain; and the University of Konstanz and Center for Psychiatry, Reichenau, Konstanz, Germany (C.W.).

Address reprint requests to Tomás Ortiz MD, PhD; Centro de Magnetoencefalografía Dr Pérez Modrego. Pabellón nº 8 Facultad de Medicina. Universidad Complutense de Madrid 28040, Madrid, Spain.

This high variability can also be found in MR imaging studies. MR imaging-based volumetric measurements seem to be among the most promising clinical tools for distinguishing patients with AD from healthy control subjects (13–16). In this case, a reduced temporoparietal and hippocampal formation volume is considered the key feature in AD. Some authors (17), emphasize the role of temporal and parietal volumes; but hippocampal, entorhinal, and parahippocampal volumes usually allow better discrimination. Juottonen et al (16) reported a sensitivity of 80% by using the volumes of left and right hippocampi and a sensitivity of 94% when entorhinal cortices were included. In a more recent study, Kiliány et al (17) obtained a discriminant function in which the volume of the entorhinal, superior temporal, and anterior cingulate cortices achieved a mean accuracy of 93%.

This state of the art suggests that isolated techniques, although certainly helpful, still cannot be used to establish a definite diagnosis of AD. As an alternative, some authors try to combine functional (PET-SPECT) measures with EEG or structural data (MR imaging) to improve the identification of AD. Yamaguchi et al (18) found significant correlations between the degree of hippocampal atrophy and the regional metabolic rate for glucose in the temporoparietal-occipital region. Buchan et al (9) reported significant negative correlations between a slow to fast EEG activity ratios (which represent the degree of slowing of the background EEG) and the regional metabolic rate for oxygen in left parietal and left and right temporal lobes. EEG findings are also correlated with the regional cerebral blood flow, with lower temporal and parietal activity associated with a decrease in alpha activity (19).

The EEG findings represent a measure of the excitatory and inhibitory postsynaptic potentials detected over the scalp. Therefore, this technique offers a highly valuable approach for assessing the pathologic neuronal changes of AD, with the exception of its lack of spatial resolution. EEG-based source localization is cumbersome, and its precision limited. These problems can be overcome with magnetic source imaging (MSI), which combines high temporal and high spatial resolution in the detection of focal neural activity (20, 21). To our knowledge, Fernández et al (22) reported the first data in which clear focal temporoparietal slow-wave activity in patients with AD was revealed by means of MSI. Moreover, this slow-wave activity was predictive of the cognitive and functional status of the patients.

Advancing this theme, MSI data have now been correlated with anatomic scores from the same sample. First, the group differences in global cerebral, hippocampal, and temporal volumes are analyzed; then the degree of correlation between increased slow-wave activity and anatomic volumes are calculated; and finally, the discrimination capability of a conjoined set of variables is determined.

Following the literature, two hypothesis are posed: 1) A strong negative correlation exists between focal

TABLE 1: Demographic data and cognitive and functional status of the sample

Measure and Group	Mean	SD
Age, y		
AD	76.27	1.21
Control	73.68	1.32
CAMCOG		
AD	55.66	6.01
Control	80.89	7.83
MMSE		
AD	19.93	2.28
Control	31.36	2.49
FAST		
AD	3.46	0.5
Control	1.36	0.59

Note.—Regarding MMSE scores, in the Spanish version by Lobo and Ezquerro (26), the maximum score is 35.

temporoparietal slow-wave generators and temporal and hippocampal levels of atrophy, and 2) discrimination between control subjects and patients with AD is improved by using a combination of functional and structural variables.

Methods

Subjects

Fifteen patients fulfilling the National Institute of Neurological and Communicative Disorders and Alzheimer's Disease and Related Disorders (23) criteria of probable AD and 16 age- and sex-matched control subjects recruited from the geriatrics unit of the Hospital Universitario San Carlos de Madrid, Spain, participated in the study. All subjects underwent general medical, neurologic, psychiatric, and psychological examinations and participated in neuroimaging studies. Patients with antecedents of post-traumatic or ischemic lesions were excluded from the study. Before the MEG recording, all subjects or legal representatives (of demented patients) provided written informed consent after we explained the technical and ethical considerations of the technique. The study was approved by the ethics committee of the Hospital Universitario San Carlos.

All subjects underwent three additional tests: functional assessment staging test (24) to evaluate their functional states, the cognitive portion of the Cambridge Examination for Mental Disorders of the Elderly (25) and the Spanish version of the Mini Mental State Examination (26) to assess their cognitive function. Table 1 summarizes the demographic data and cognitive and functional status of the subjects.

MEG Data Collection and Analysis

MEG data were measured by using a 148-channel whole-head magnetometer (Magnes 2500 WH; 4D Neuroimaging, San Diego, CA) during a 10-minute resting period. Recordings were obtained with the subjects lying down, and they were asked to stay awake and to avoid head and eye movement by fixing their gaze on a black point on the ceiling. To avoid and control drowsiness effects, subjects' behavior and level of consciousness was monitored during the entire recording by using a video camera. The MEG was recorded with a 678.17-Hz sampling rate by using a band-pass filter of 0.1–200 Hz. Eye movements were recorded from four electrodes attached to the left and right outer canthus and above and below the left eye. The electrocardiogram was monitored with electrodes attached to the right collarbone and to the lowest left rib. Each 10-

minute data set was decimated (which consisted of filtering the data to be consistent with Nyquist criteria [27], followed by a downsampling by a factor of 16). The band-pass was filtered before the analysis in the delta (1.5–4.0-Hz) and theta (4.0–8.0-Hz) bands. Dipole density (DD) was estimated on the basis of an equivalent current dipole in a homogeneous sphere calculated for each time step.

Artifact-free time segments of varying lengths were determined by visual inspection. Single equivalent dipoles were fitted for each time point in the selected epochs. The location of activity sources was computed with reference to a Cartesian coordinate system defined by a set of three anatomic landmarks (fiducial points): the right and left external meatus and the nasion. The position of the magnetometers relative to the subject's head was precisely determined by using five coils, three of which were attached to the fiducial points and two to the forehead. The coils were activated briefly at the beginning of the recording session and again at the end, and their precise location in three-dimensional space was determined by using a localization algorithm built into the system. During the recording session, a fiberoptic motion detector was used to ensure that the subjects' head did not change position relative to the sensor.

Only dipole fit solutions at time points with a root mean square over 100 fT and a goodness of fit over 0.90 were accepted for further analysis. Root mean square was determined by using the equation $RMS = \sqrt{1/n \sum x_i^2}$, where n represents total number of data points and x_i , measured field value in each data point. For statistical analysis, the total brain volume was divided into 10 regions representing the frontal, parietal, prefrontal, temporal, and occipital areas in both hemispheres, and the number of successful dipole fits was determined for each of these regions (28). The total number of dipoles per second that fit the criteria in the delta and theta bands was determined for each subject and region. To avoid the possible influence of the individual time-segment lengths over the DD scores, the raw number of dipoles per region was normalized by using the following equation: Number of dipoles per second = raw number of dipoles/sampling rate \times absolute number of recorded points, where the absolute number of recorded points is the final number of recorded points after the artifacts are eliminated. This number of dipoles per second per region was the final score used for the statistical analysis.

MR Imaging–Volumetry

High-resolution three-dimensional (3D) volume images were acquired from each subject with a 1.5-T unit (Signa; GE Medical Systems, Milwaukee, WI). T1-weighted images (TR/TE/NEX, 14.6/3.1/1; flip angle, 15°) were obtained by using gradient-echo (3D-SPGR) sequences with a field of view of 22 \times 16.5 cm, a 256 \times 194 matrix, and 1-mm section thickness. The entire brain and skull were covered in the axial plane. The voxel size was 0.7 mm³. The volumetric measurements were performed with the RM Tissue Volume software (GE Medical Systems) running in an Advantage Windows 4.0 environment. Regions of interest on each image were defined by using the Semi-Automatic Volume Segmentation protocol (3SAVS) that is part of the software. This software allows the user to draw a region of interest in each section with the mouse, assisted by border attraction and 3D automatic paint tools, and to measure the volume of the painted region (in cubic centimeters). After the measures are obtained, the software allows the operator to gather a histogram of the voxel value for the region of interest. The following regions of interest were defined: total cranial volume (TCrV), total cerebral volume (TCV), right hippocampal volume (RHV) and left hippocampal volume (LHV), right (RTV) and left lateral temporal lobe (LTV) volume.

In accordance with the procedure of Kidron et al (15), the entire volume of the brain, including the brain stem and cerebellum, was calculated from the edited brain as an index of the total intracranial capacity. Then, on the lateral surface of the

hemispheres, the sylvian fissure was traced, and the parieto-occipital fissure and the preoccipital notch were identified and joined by a line. A line was drawn from the posterior end of the sylvian fissure to the line joining the parieto-occipital fissure and the preoccipital notch to provide the posterior demarcation of the temporal lobe. Hippocampal anatomic boundaries were defined to include the CA1–CA4 sectors of the hippocampus, the dentate gyrus, and the subiculum. The posterior boundary of the hippocampus was determined by the oblique coronal anatomic section on which the crura at the fornices were identified in full profile. Thus, the entire hippocampus from the tail through the head was included in the measurements.

The ratio of total cerebral to total cranial volume (relative cerebral volume [TCVr]) was then calculated according to the formula: $TCVr = TCV/TCrV$. In a similar manner, we computed the proportion of the total cranial volume represented by the right (RHVr) and left hippocampal (LHVr), and the right (RTVr) and left (LTVr) temporal volumes. Only relative measures were used in the statistical analyses to control for possible group differences in brain size (29).

For reliability assessment of the MR imaging measures, the agreement of two independent neuroradiologists (J.A.) blinded to the clinical and MEG results was evaluated. The mean difference between the two observers for the left hippocampus was -0.03 (95% confidence interval: $-0.14, 0.08$) and 0.07 for the right (95% confidence interval: $-0.3, 0.1$). Similar results were found for the left temporal area, -0.07 (95% confidence interval: $-0.11, 0.09$) and for the right, 0.09 (95% confidence interval: $-0.7, 0.2$). Interrater reliabilities were high (left hippocampus, $r = 0.99$; right hippocampus, $r = 0.98$; left temporal, $r = 0.97$; right temporal, $r = 0.98$).

All the units used for the structural data were cubic centimeters.

Results

Volumetric MR imaging Analyses: Group Effects

Figures 1 and 2 display the relative cerebral and hippocampal volumes in a patient with AD. A series of mean comparisons (Student t tests) between groups was performed on the MR imaging volumetric variables. Given a total number of five comparisons (TCVr, RHVr, LHVr, RTVr, LTVr), an adjusted α level of $0.05/5 = 0.01$ was used to evaluate each t test according to the Bonferroni method. The AD group had lower volumes than the elderly control group in cerebral volume, with these values: $t(29) = -4.066$, $P < .0001$; left, $t(29) = -6.604$, $P < .0001$; and right hippocampus, $t(14) = 5.255$, $P < .0001$. The two groups did not differ in the other relative volume measures.

Correlation between Volumetric MR Imaging Data and MEG Data

Pearson correlation coefficients were computed between the MR imaging volumetric variables and seven MEG-based activity measures were used that represented the DD sources in the left and right parietal lobes and left temporal lobe for delta band activity and those in the parietal and temporal, both left and right-sided, for theta band sources. These MEG-based variables correspond to the previously defined significant factors that enable a correct discrimination of AD and control subjects (22). Table 2

FIG 1. T1-weighted MR images display the relative global cerebral volume in a patient with AD in axial and sagittal views. Green represents the final region where the volume calculation was performed.

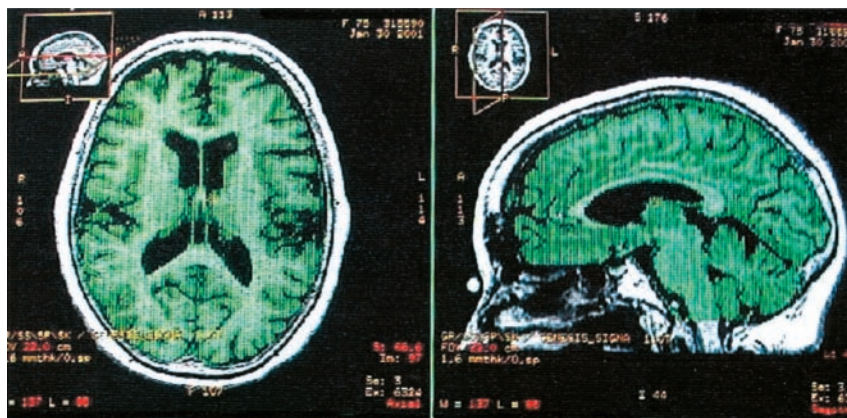
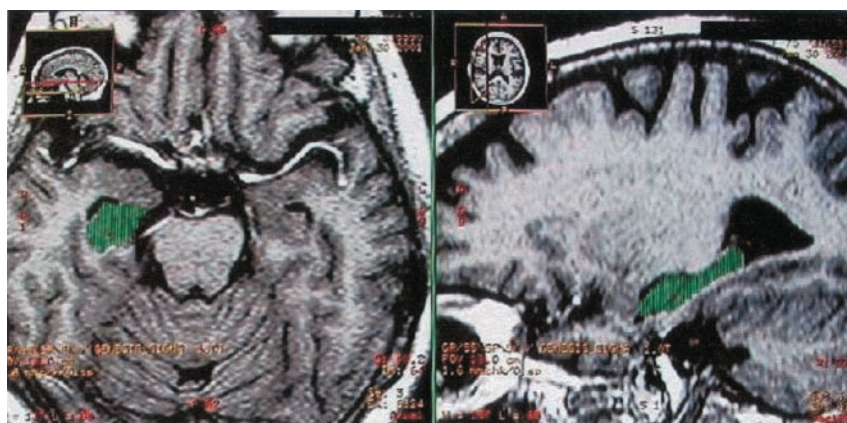


FIG 2. T1-weighted MR images display the relative hippocampal volume in a patient with AD in the axial and sagittal planes. Green represents the final region where the volume calculation was performed.



shows the DD values of the ten regions for delta and theta bands obtained in the previous study. A total of 35 correlation coefficients were computed (between each of the seven MEG variables and each of the five MR imaging variables) and evaluated by using a Bonferroni-corrected α level of $0.05/35 = 0.002$. Although a considerable number of negative correlations between the MEG variables and left temporal relative volume, and relative bilateral hippocampal volume were found (Table 3), only three coefficients reached statistical significance: those between relative volume of the left hippocampus and left parietal delta DD, left temporal delta DD, and left parietal theta DD. This observation indicates that the higher the number of low-frequency activity sources in left temporal and parietal areas, the higher the atrophy in the mesial aspects of the left temporal lobe.

Conjunct Volumetric MR Imaging–MEG Discriminative Capability: Discriminant Analysis

A discriminant analysis including the aforementioned seven MEG and five MR imaging variables was performed to clarify the relationship between two different techniques (ie, volumetric MR imaging and MEG) and their ability to improve the diagnosis of AD.

This discriminant analysis was used to classify subjects in the AD or control group on the basis of a discriminant function by using only two variables. In order of entry, the variables were LHVR and left temporal theta DD. Applying the weights obtained from

this analysis to the cross-validation sample, three controls and one AD patient were classified incorrectly; the total correct classification rate was 87.1% (Table 4). The formula of the discriminant function obtained in this analysis was expressed in terms of standardized coefficients: Canonical variable = $(0.948)\text{LHVR} - (0.451)\text{left temporal theta DD}$.

Those with canonical scores equal to or greater than 0 were classified as control subjects, whereas those with canonical scores below 0 were classified as patients with AD (Figs 3 and 4).

Discussion

The present results support the previous hypothesis that relative global cerebral and hippocampal volumes are significantly lower in AD groups compared with those in control subjects, whereas the relative temporal volumes do not differ between groups. Global cerebral atrophy (including ventricular and fissural enlargement) is a common finding in AD; it progressively affects the mesial temporal and association areas, sparing the primary motor and sensory cortices (30, 31). However, the atrophy due to normal aging is difficult to distinguish from the specific atrophy due to AD, and this difficulty explains part of the contradictory findings reported in the literature. Ohmishi et al (32) performed one of the most detailed analyses of the age-related cerebral volume decline versus AD-related cerebral volume decline. Healthy volunteers had a clear age-related decrease

TABLE 2: Means and SDs of the 10 MEG DD variables for delta and theta bands

Variable	Delta Band		Variable	Theta Band	
	Mean	SD		Mean	SD
A: AD group					
LF_D	.406	.094	LF_T	.868	.221
RF_D	.327	.079	RF_T	.811	.294
LP_D	1.190*	.209	LP_T	1.959*	.333
RP_D	.982*	.162	RP_T	2.418*	.405
LPF_D	.794	.174	LPF_T	.682	.146
RPF_D	.604	.175	RPF_T	.410	.117
LT_D	.313*	.071	LT_T	.531*	.119
RT_D	.225	.059	RT_T	.833*	.185
LO_D	.219	.108	LO_T	.320	.145
RO_D	.256	.093	RO_T	.328	.106
B: Control group					
LF_D	.213	.091	LF_T	.545	.214
RF_D	.193	.076	RF_T	.395	.284
LP_D	.354	.202	LP_T	.884	.322
RP_D	.288	.157	RP_T	.879	.392
LPF_D	.435	.168	LPF_T	.454	.141
RPF_D	.459	.169	RPF_T	.381	.113
LT_D	6.140E-02	.068	LT_T	.141	.115
RT_D	6.284E-02	.057	RT_T	.189	.180
LO_D	4.439E-02	.105	LO_T	.225	.141
RO_D	7.432E-02	.090	RO_T	.178	.103

Note.—Abbreviations are as follows: LF_D, left frontal delta; RF_D, right frontal delta; LP_D, left parietal delta; RP_D, right parietal delta; LPF_D, left prefrontal delta; RPF_D, right prefrontal delta; LT_D, left temporal delta; RT_D, right temporal delta; LO_D, left occipital delta; RO_D, right occipital delta; LF_T, left frontal theta; RF_T, right frontal theta; LP_T, left parietal theta; RP_T, right parietal theta; LPF_T, left prefrontal theta; RPF_T, right prefrontal theta; LT_T, left temporal theta; RT_T, right temporal theta; LO_T, left occipital theta; and RO_T, right occipital theta.

* Variables with significant differences between groups. For more information, see Fernández et al (22).

TABLE 3: Correlation coefficients between MEG and MRI variables

MEG Variable	MRI Variable				
	CVr	RTVr	LTVr	RHVr	LHVr
Left parietal_delta	-.35*	-.23	-.35 [†]	-.42*	-.47 [§]
Right parietal_delta	-.26	-.25	-.39 [†]	-.37 [†]	-.41*
Left temporal_delta	-.29	-.12	-.21	-.33*	-.46 [§]
Left parietal_theta	-.38 [†]	-.25	-.37 [§]	-.40 [§]	-.44 [§]
Right parietal_theta	-.29	-.20	-.30	-.26	-.34
Left temporal_theta	-.34*	-.26	-.29	-.31*	-.40 [§]
Right temporal_theta	-.11	-.23	-.30	-.21	-.022

* $P < .05$.

[†] $P < .025$.

[‡] $P < .01$.

[§] $P < .002$.

in the volumes of the prefrontal cortex, insula, anterior cingulate gyrus, superior temporal gyrus, and inferior parietal lobule. The authors considered that these changes may promote some cognitive alterations during normal aging, but only a significant

TABLE 4: Results of discriminant analysis classification

Group	Predicted Group		Total
	AD	Control	
Original			
Count			
AD	12	3	15
Control	1	15	16
Ungrouped cases	3	5	8
Percentage, %			
AD	80.0	20.0	100.0
Control	6.3	93.8	100.0
Ungrouped cases	37.5	62.5	100.0
Cross-validated			
Count			
AD	12	3	15
Control	1	15	16
Percentage, %			
Alzheimer	80.0	20.0	100.0
Control	6.3	93.8	100.0

bilateral reduction of gray matter volume in the hippocampal formation and entorhinal cortex explained the pathologic characteristics for AD and definitively defined this group. Many different studies support the evidence of the hippocampal atrophy as the critical structural feature of AD, even during the earliest stages of the disease (33–36). This hippocampal deficit is usually accompanied by entorhinal, perirhinal, amygdalar, or parahippocampal alterations (17, 36) that contribute to the role of the mesial temporal lobe (MTL) in the diagnosis of AD.

Our data support these findings, not only because relative hippocampal volumes reflect substantial differences between the groups but also because only these volumes were significantly correlated with low-frequency temporoparietal DD. As described before, hippocampal atrophy is correlated with temporoparietal-occipital hypometabolism (18). Additionally, mirroring the results of Dierks et al (10), who consider glucose metabolism and neuroelectric activity to be reflections of synaptic activity, and those of Buchan et al (9), a strong correlation between focal temporoparietal low-frequency neuromagnetic activity and hippocampal atrophy could be predicted as well. Although EEG (37) or even MEG (38) investigations may provide congruent data, the findings seem to be anatomically less precise.

The primary consideration emerging from comparison of the present results and those in the previous literature is that three brain regions represent the most common anatomic landmarks affected by AD: the mesial temporal, the temporal, and the parietal lobes. MTL atrophy is probably the most sensitive measure in the structural approach, and it may be useful in detecting AD-specific alterations, even in the earliest stages of the disease. Temporoparietal hypofunctioning defined by means of metabolic, neuroelectric, or neuromagnetic techniques is the most sensitive functional measure. Moreover, functional and structural data demonstrate strong relationships in many ways; consequently, the

FIG 3. Histogram representing the results of the discriminant analysis for the Alzheimer group: x axis reflects canonical scores, and y axis reflects the number of subjects who obtained every canonical score. Those with canonical scores below zero were classified as belonging to the AD group; three controls were incorrectly classified within the AD group.

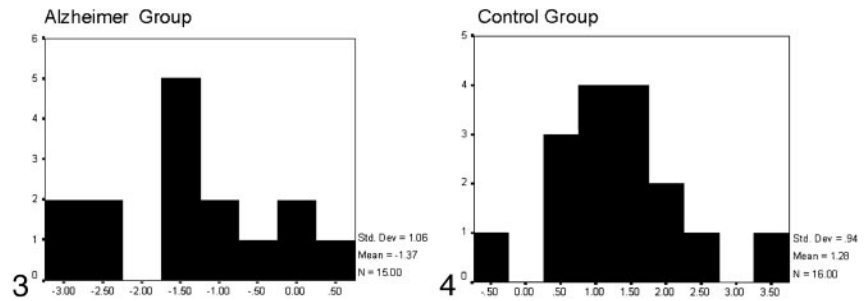


FIG 4. Histogram representing the results of the discriminant analysis for the control group: x axis reflects canonical scores, and y axis reflects the number of subjects who obtained every canonical score. Those with canonical scores greater than zero were classified as controls; one AD patient was incorrectly classified as belonging to the control group.

combination of both approaches may contribute to better identification of AD.

Discriminant analysis elucidates how a combination of structural (LHVr) and functional (left temporal theta DD) data provides a substantial level of discriminant capability. An 87.1% rate of correct classification is a score superior to the median of 81% observed in singular SPECT or EEG studies (5, 12). Many of these studies involved relatively small numbers of patients. Juottonen et al (16) pointed out that the probability of overlap between control subjects and patients with AD increases with the sample size. They explained this stable effect in terms of the diagnostic weakness of AD. Results of pathologic studies suggest that some neuropathologic changes (including atrophy and neural hypofunctioning) might appear before the clinical diagnosis is made; therefore, the overlap could be due to an incipient AD in some control subjects. In fact, our results might confirm this hypothesis because the main source of classification error is derived from three control subjects who were incorrectly classified as having AD. As previously demonstrated (22), low-frequency DD is strongly correlated with the neuropsychological data and partially explains their variability. Control subjects with lower cognitive and functional scores present with higher levels of low-frequency activity, and therefore, the risk of misclassification among these individuals increases.

The origin of the strong relationship between the structural integrity of the MTL structures and the functional status of temporoparietal areas in AD remain to be explained. We suggest two different but closely related explanations: First, AD is a pervasive degenerative disease in which MTL alterations are often, but not always, considered the preliminary manifestations. With disease progression, temporoparietal and, eventually, frontal regions are affected (33). However, the interindividual variability in the evolution of the disease, and some technical limitations, may contribute to the fact that different studies help in detecting different stages of the same process given the unique sensitivity of each technique. On the other hand, Killiany et al (17) and Lavenex and Amaral (39) claim that the early degenerative changes in the entorhinal cortex impair critical functional connections between the temporoparietal neocortex and the hippocampal formation. A disconnec-

tion between the MTL structures and the neocortical areas in the ipsilateral hemisphere could seriously harm the circuitry of the association cortices in terms of functional activation. Therefore, MTL atrophy and temporoparietal hypofunctioning could be considered complementary pictures of the same involutive process.

Conclusion

The results of this study supports the idea that a combination of complementary techniques (ie, functional MEG and structural MR imaging) and improved clinical diagnosis will improve our understanding of AD and permit better detection of the disease.

Acknowledgments

This study was supported in part by 4-D Neuroimaging. The authors would like to thank to Thomas Murphy for his technical support with MEG.

References

1. Jagust WJ, Budinger TF, Reed B. The diagnosis of dementia with single photon emission computed tomography. *Arch Neurol* 1987; 44:258-262
2. Jagust WJ, Eberling JL, Reed BR, Mathis CA, Budinger TF. Clinical studies of cerebral blood flow in Alzheimer's disease. *Ann NY Acad Sci* 1997;826:254-262
3. Jagust WJ, Haan MN, Reed BR, Eberling JL. Brain perfusion imaging predicts survival in Alzheimer's disease. *Neurology* 1998; 51:1009-1013
4. Neary D, Snowden JS, Shields RA. Single photon emission tomography using ^{99m}Tc -HM-PAO in the investigation of dementia. *J Neurol Neurosurg Psychiatry* 1987;50:1101-1119
5. Talbot PR, Lloyd JJ, Snowden JS. A clinical role for ^{99m}Tc -HM-PAO SPECT in the investigation of dementia? *J Neurol Neurosurg Psychiatry* 1998;64:306-313
6. Masterman DL, Mendez MF, Fairbanks LA. Sensitivity, specificity, and positive predictive value of technetium 99-HMPAO SPECT in discriminating Alzheimer's disease from other dementias. *J Geriatr Psychiatry Neurol* 1997;10:15-21
7. Rapoport SI. Positron emission tomography in Alzheimer's disease in relation to disease pathogenesis: a critical review. *Cerebrovasc Brain Metab* 1991;3:297-335
8. Van Gool WA, Walstra GJ, Teunisse S. Diagnosing Alzheimer's disease in elderly, mildly demented patients: the impact of routine single photon emission computed tomography. *J Neurol* 1995;242: 401-405
9. Buchan RJ, Nagata K, Yokoyama E, et al. Regional correlations between the EEG and oxygen metabolism in dementia of the Alzheimer's type. *Electroencephalogr Clin Neurophysiol* 1997;103:409-417
10. Dierks T, Jelic V, Pascual-Marqui RD, et al. Spatial pattern of

- cerebral glucose metabolism (PET) correlates with localization of intracerebral EEG-generators in Alzheimer disease. *Clin Neurophysiol* 2000;111:1817–1824
11. Matousek M, Brunovsky M, Edman A, Wallin A. EEG abnormalities in dementia reflect the parietal lobe syndrome. *Clin Neurophysiol* 2001;112:1001–1005
 12. Jonkman EJ. The role of the electroencephalogram in the diagnosis of dementia of the Alzheimer type: an attempt at technology assessment. *Neurophysiol Clin* 1997;27:211–219
 13. De Carli C, Murphy DGM, McIntosh AR, Teichberg D, Schapiro MB, Horwitz B. Discriminant analysis of MRI measures as a method to determine the presence of dementia of the Alzheimer type. *Psychiatry Res* 1995;57:119–130
 14. Laakso MP, Soininen H, Partanen K. Volumes of hippocampus, amygdala and frontal lobes in the MRI-based diagnosis of early Alzheimer's disease: correlation with memory functions. *J Neural Transm* 1995;9:73–86
 15. Kidron D, Black SE, Stanev P, et al. Quantitative MR volumetry in Alzheimer's disease. Topographic markers and the effect of sex and education. *Neurology* 1997;49:1504–1512
 16. Juottonen K, Laakso MP, Partanen K, Soininen H. Comparative MR analysis of the entorhinal cortex and hippocampus in diagnosing Alzheimer disease. *AJNR Am J Neuroradiol* 1999;20:139–144
 17. Killiany RJ, Gomez-Isla T, Moss M, Kikinis R, Sandor T, Jolesz F. Use of structural magnetic resonance imaging to predict who will get Alzheimer's disease. *Ann Neurol* 2000;47:430–439
 18. Yamaguchi S, Meguro K, Itoh M, et al. Decreased cortical glucose metabolism correlates with hippocampal atrophy in Alzheimer's disease as shown by MRI and PET. *J Neurol Neurosurg Psychiatry* 1997;62:596–600
 19. Claus JJ, Ongerboer De Visser BW, et al. Determinants of quantitative spectral electroencephalography in early Alzheimer's disease: cognitive function, regional cerebral blood flow, and computed tomography. *Dementia Geriatr Cogn Disord* 2000;11:81–89
 20. Elbert T. Neuromagnetism. In: Andr  W, Nowak H, eds. *Magnetism in Medicine*. New York: J Wiley & Sons, 1998;190–262
 21. Vieth J, Kober H, Grummich P. Slow wave and beta wave activity associated with white matter structural brain lesions, localized by the dipole density plot. In: Baumgartner C, Deecke L, Stroink G, Willianson SJ, eds. *Biomagnetism: Fundamental Research and Clinical Applications*. Amsterdam: Elsevier/IOS-Press; 1995;50–54
 22. Fern ndez A, Maest  F, Amo C, et al. Focal temporo-parietal slow activity in Alzheimer's disease revealed by magnetoencephalography. *Biol Psychiatry*. In press.
 23. McKhann G, Drachman D, Folstein M, et al. Clinical diagnosis of Alzheimer's disease: report of NINCDS-ADRDA work group under the auspices of department of health and human services task force on Alzheimer's disease. *Neurology* 1984;34:939–944
 24. Reisberg B. Functional assessment staging (FAST). *Psychopharmacol Bull* 1988;24:653–659
 25. Roth M, Huppert FA, Tym E, Mountjoy CQ. *CAMDEX, the Cambridge Examination for Mental Disorders of the Elderly*. Cambridge: Cambridge University Press; 1988
 26. Lobo A, Ezquerro V. El mini-examen cognoscitivo: un test sencillo y pr ctico para detectar alteraciones intelectivas en pacientes m dicos. *Actas Luso-Esp  ol Psiquiatr  Psicol M d* 1979;3:189–202
 27. Oppenheim AV, Schaffer RW. *Digital Signal Processing*. Englewood Cliffs: Prentice-Hall; 1974
 28. Fehr T, Kissler J, Moratti S, Wienbruch C, Rockstroh B, Elbert T. Source distribution of neuromagnetic slow waves and MEG-delta activity in Schizophrenic patients. *Biol Psychiatry* 2001;50:108–116
 29. Whitwell JL, Crum WR, Watt HC, Fox NC. Normalization of cerebral volumes by use of intracranial volume: implications for longitudinal quantitative MR imaging. *AJNR Am J Neuroradiol* 2001;22:1483–1489
 30. Mori E, Yoneda Y, Yamashita H, Hirono N, Ikeda M, Yamadori A. Medial temporal structures relate to memory impairment in Alzheimer's disease. *J Neurol, Neurosurg Psychiatry* 1997;63:214–221
 31. Thompson PM, Mega MS, Woods RP, et al. Cortical change in Alzheimer's disease detected with a disease-specific population-based brain atlas. *Cereb Cortex* 2001;11:1–16
 32. Ohmishi T, Matsuda H, Tabira T, Asada T, Uno M. Changes in brain morphology in Alzheimer disease and normal aging: is Alzheimer disease an exaggerated aging process? *AJNR Am J Neuroradiol* 2001;22:1680–1685
 33. Jack CR, Petersen RC, Xu YC, et al. Medial temporal atrophy on MRI in normal aging and very mild Alzheimer's disease. *Neurology* 1997;49:786–794
 34. Lehericy S, Baulac M, Chiras J. Amygdalohippocampal MR volume measurements in the early stages of Alzheimer disease. *AJNR Am J Neuroradiol* 1994;15:927–937
 35. Convit A, De Le n MJ, Golomb J, George AE. Hippocampal atrophy in early Alzheimer's disease: anatomic specificity and validation. *Psychiatry Q* 1993;64:371–387
 36. Convit A, De Le n MH, Tarshish C. Hippocampal volume losses in minimally impaired elderly. *Lancet* 1995;345:266
 37. F rstl H, Besthorn C, S ttle H, et al. Volumetric brain changes and quantitative EEG in normal aging and Alzheimer's disease. *Nervenarzt* 1996;67:53–61
 38. Berendse HW, Verbunt JPA, Scheltens P, Van Dijk BW, Jonkman EJ. Magnetoencephalographic analysis of cortical activity in Alzheimer's disease: a pilot study. *Clin Neurophysiol* 2000;111:604–612
 39. Lavenex P, Amaral DG. Hippocampal-neocortical interaction: a hierarchy of associativity. *Hippocampus* 2000;10:420–430